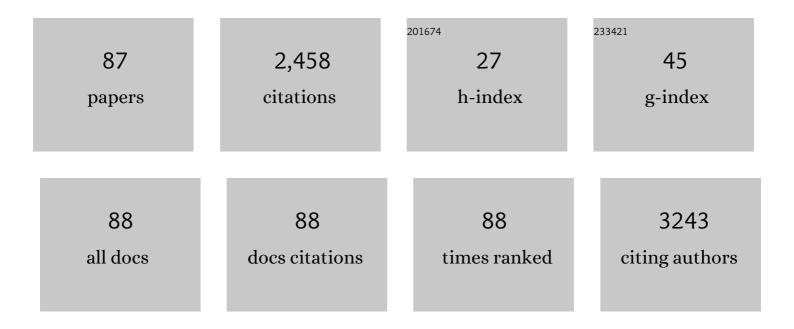
List of Publications by Year in descending order

Source: https://exaly.com/author-pdf/11820885/publications.pdf Version: 2024-02-01



#	Article	IF	CITATIONS
1	Magnetophoretic Microâ€Distributor for Controlled Clustering of Cells. Advanced Science, 2022, 9, e2103579.	11.2	8
2	Advances and key technologies in magnetoresistive sensors with high thermal stabilities and low field detectivities. APL Materials, 2022, 10, .	5.1	14
3	Tailoring matter orbitals mediated using a nanoscale topographic interface for versatile colloidal current devices. Materials Horizons, 2022, 9, 2353-2363.	12.2	4
4	The trajectory of bio-carriers in periodic energy landscape regulated by the multiple collision history in a magnetophoretic system. Journal of Science: Advanced Materials and Devices, 2022, 7, 100482.	3.1	2
5	Highly sensitive electrochemical biosensor based on naturally reduced rGO/Au nanocomposite for the detection of miRNA-122 biomarker. Journal of Industrial and Engineering Chemistry, 2021, 93, 186-195.	5.8	65
6	Microvalve-controlled miniaturized electrochemical lab-on-a-chip based biosensor for the detection of β-amyloid biomarker. Journal of Industrial and Engineering Chemistry, 2021, 97, 349-355.	5.8	10
7	Magnetophoretic Decoupler for Disaggregation and Interparticle Distance Control. Advanced Science, 2021, 8, 2100532.	11.2	9
8	Mattertronics for programmable manipulation and multiplex storage of pseudo-diamagnetic holes and label-free cells. Nature Communications, 2021, 12, 3024.	12.8	19
9	Operational Parameters for Sub-Nano Tesla Field Resolution of PHMR Sensors in Harsh Environments. Sensors, 2021, 21, 6891.	3.8	3
10	Real-time monitored photocatalytic activity and electrochemical performance of an rGO/Pt nanocomposite synthesized <i>via</i> a green approach. RSC Advances, 2020, 10, 13722-13731.	3.6	13
11	Performance Validation of a Planar Hall Resistance Biosensor through Beta-Amyloid Biomarker. Sensors, 2020, 20, 434.	3.8	12
12	Phase controlled one-pot synthesis of heterostructured FePt–Fe3O4 nanocubes with excellent biocompatibility. RSC Advances, 2020, 10, 43480-43488.	3.6	3
13	Reduced thermal dependence of the sensitivity of a planar Hall sensor. Applied Physics Letters, 2019, 115, .	3.3	17
14	Multifarious Transit Gates for Programmable Delivery of Bioâ€functionalized Matters. Small, 2019, 15, e1901105.	10.0	11
15	Equisensitive adjustment of planar Hall effect sensor's operating field range by material and thickness variation of active layers. Journal Physics D: Applied Physics, 2019, 52, 285001.	2.8	13
16	Magnetically Characterized Molecular Lubrication between Biofunctionalized Surfaces. ACS Applied Materials & Interfaces, 2018, 10, 16177-16182.	8.0	10
17	Scalable production of water-dispersible reduced graphene oxide and its integration in a field effect transistor. Journal of Industrial and Engineering Chemistry, 2018, 63, 19-26.	5.8	14
18	Characterization of Superparamagnetic Particles Mobility by On-Chip Micromagnets. IEEE Transactions on Magnetics, 2018, 54, 1-4.	2.1	2

#	Article	IF	CITATIONS
19	Free and forced Barkhausen noises in magnetic thin film based cross-junctions. Journal of Magnetism and Magnetic Materials, 2018, 458, 292-300.	2.3	12
20	Effect of NiFeCr seed and capping layers on exchange bias and planar Hall voltage response of NiFe/Au/IrMn trilayer structures. Journal of Applied Physics, 2018, 123, .	2.5	13
21	Autonomous Magnetic Microrobots by Navigating Gates for Multiple Biomolecules Delivery. Small, 2018, 14, e1800504.	10.0	17
22	Ultra-sensitive 2-nitrophenol detection based on reduced graphene oxide/ZnO nanocomposites. Journal of Electroanalytical Chemistry, 2017, 788, 66-73.	3.8	72
23	Multifunctional Fe ₃ O ₄ /Au core/satellite nanocubes: an efficient chemical synthesis, characterization and functionalization of streptavidin protein. Dalton Transactions, 2017, 46, 2303-2309.	3.3	18
24	A novel and rapid approach for the synthesis of biocompatible and highly stable Fe ₃ O ₄ /SiO ₂ and Fe ₃ O ₄ /C core/shell nanocubes and nanorods. New Journal of Chemistry, 2017, 41, 2724-2734.	2.8	14
25	Concentric manipulation and monitoring of protein-loaded superparamagnetic cargo using magnetophoretic spider web. NPG Asia Materials, 2017, 9, e369-e369.	7.9	22
26	Highly sensitive and selective detection of Bis-phenol A based on hydroxyapatite decorated reduced graphene oxide nanocomposites. Electrochimica Acta, 2017, 241, 353-361.	5.2	52
27	Nano/micro-scale magnetophoretic devices for biomedical applications. Journal Physics D: Applied Physics, 2017, 50, 033002.	2.8	38
28	Magnetic Susceptibility Study of Subâ€Picoâ€emu Sample Using a Micromagnetometer: An Investigation through Bistable Spinâ€Crossover Materials. Advanced Materials, 2017, 29, 1703073.	21.0	22
29	Hierarchical gold nanostructures modified electrode for electrochemical detection of cancer antigen CA125. Sensors and Actuators B: Chemical, 2017, 243, 64-71.	7.8	71
30	Remote tactile sensing system integrated with magnetic synapse. Scientific Reports, 2017, 7, 16963.	3.3	23
31	Role of Spin on Future Biomedical Science: Logical Manipulation of Living Cells for Novel Cells-On-Chip. , 2016, , .		0
32	An on-chip micromagnet frictionometer based on magnetically driven colloids for nano-bio interfaces. Lab on A Chip, 2016, 16, 3485-3492.	6.0	23
33	Electrochemical biosensor for Mycobacterium tuberculosis DNA detection based on gold nanotubes array electrode platform. Biosensors and Bioelectronics, 2016, 78, 483-488.	10.1	67
34	Morphology-controlled synthesis of highly crystalline Fe ₃ O ₄ and CoFe ₂ O ₄ nanoparticles using a facile thermal decomposition method. RSC Advances, 2016, 6, 15861-15867.	3.6	61
35	Dynamic trajectory analysis of superparamagnetic beads driven by on-chip micromagnets. Journal of Applied Physics, 2015, 118, 203904.	2.5	24
36	Protein immobilization onto electrochemically synthesized CoFe nanowires. International Journal of Nanomedicine, 2015, 10, 645.	6.7	12

#	Article	IF	CITATIONS
37	Size controlled sonochemical synthesis of highly crystalline superparamagnetic Mn–Zn ferrite nanoparticles in aqueous medium. Journal of Alloys and Compounds, 2015, 644, 774-782.	5.5	22
38	Facile one-pot chemical approach for synthesis of monodisperse chain-like superparamagnetic maghemite (Î ³ -Fe2O3) nanoparticles. Journal of Industrial and Engineering Chemistry, 2015, 31, 43-46.	5.8	16
39	A novel approach for the synthesis of ultrathin silica-coated iron oxide nanocubes decorated with silver nanodots (Fe ₃ O ₄ /SiO ₂ /Ag) and their superior catalytic reduction of 4-nitroaniline. Nanoscale, 2015, 7, 12192-12204.	5.6	93
40	Planar Hall ring sensor for ultra-low magnetic moment sensing. Journal of Applied Physics, 2015, 117, .	2.5	24
41	Facile approach for synthesis of high moment Fe/ferrite and FeCo/ferrite core/shell nanostructures. Materials Letters, 2015, 139, 161-164.	2.6	24
42	Thermal annealing synthesis of Fe4N/Fe nanocomposites from iron oxide (Fe3O4) nanoparticles. Journal of the Korean Physical Society, 2014, 65, 1649-1652.	0.7	2
43	Modified polyol route for synthesis of Fe3O4/Ag and α-Fe/Ag nanocomposite. Journal of Alloys and Compounds, 2014, 615, S308-S312.	5.5	13
44	Highly stable- silica encapsulating magnetite nanoparticles (Fe3O4/SiO2) synthesized using single surfactantless- polyol process. Ceramics International, 2014, 40, 1379-1385.	4.8	97
45	Size-controlled high magnetization CoFe2O4 nanospheres and nanocubes using rapid one-pot sonochemical technique. Ceramics International, 2014, 40, 3269-3276.	4.8	70
46	Magnetophoretic circuits for digital control of single particles and cells. Nature Communications, 2014, 5, 3846.	12.8	104
47	Optimization of magnetic switches for single particle and cell transport. Journal of Applied Physics, 2014, 115, .	2.5	15
48	Ultrasonic manipulation of magnetic particles in a microfluidic channel. International Journal of Precision Engineering and Manufacturing, 2014, 15, 1411-1416.	2.2	3
49	Fe3O4/TiO2 core/shell nanocubes: Single-batch surfactantless synthesis, characterization and efficient catalysts for methylene blue degradation. Ceramics International, 2014, 40, 11177-11186.	4.8	120
50	Shape and size-controlled synthesis of Ni Zn ferrite nanoparticles by two different routes. Materials Chemistry and Physics, 2014, 147, 443-451.	4.0	49
51	Synthesis of monodisperse and high moment nickel–iron (NiFe) nanoparticles using modified polyol process. Current Applied Physics, 2013, 13, 2010-2013.	2.4	15
52	Biosynthesis of Gold Nanoparticles Assisted by <i>Sapindus mukorossi</i> Gaertn. Fruit Pericarp and Their Catalytic Application for the Reduction of <i>p</i> -Nitroaniline. Industrial & Engineering Chemistry Research, 2013, 52, 556-564.	3.7	118
53	Room Temperature Magnetic Detection of Spin Switching in Nanosized Spin rossover Materials. Angewandte Chemie - International Edition, 2013, 52, 1185-1188.	13.8	37
54	Planar Hall resistance ring sensor based on NiFe/Cu/IrMn trilayer structure. Journal of Applied Physics, 2013, 113, .	2.5	31

#	Article	IF	CITATIONS
55	Optimization of Pathway Pattern Size for Programmable Biomolecule Actuation. IEEE Transactions on Magnetics, 2013, 49, 408-413.	2.1	11
56	Synthesis of high magnetization hydrophilic magnetite (Fe3O4) nanoparticles in single reaction—Surfactantless polyol process. Ceramics International, 2013, 39, 7605-7611.	4.8	78
57	Facile sonochemical synthesis of high-moment magnetite (Fe3O4) nanocube. Journal of Nanoparticle Research, 2013, 15, 1.	1.9	76
58	NiCo sensing layer for enhanced signals in planar hall effect sensors. Metals and Materials International, 2013, 19, 875-878.	3.4	5
59	An organic substrate based magnetoresistive sensor for rapid bacteria detection. Biosensors and Bioelectronics, 2013, 41, 758-763.	10.1	27
60	One-pot synthesis of high magnetization air-stable FeCo nanoparticles by modified polyol method. Materials Letters, 2013, 91, 326-329.	2.6	63
61	Silica encapsulation of sonochemically synthesized iron oxide nanoparticles. Electronic Materials Letters, 2013, 9, 817-820.	2.2	12
62	Micro-magnetometry for susceptibility measurement of superparamagnetic single bead. Sensors and Actuators A: Physical, 2012, 182, 34-40.	4.1	29
63	Ultrasonic alignment of bio-functionalized magnetic beads and live cells in PDMS micro-fluidic channel. Biomedical Microdevices, 2012, 14, 1077-1084.	2.8	6
64	Effect of magnetic field on the dielectric properties of multiferroic composites. Journal of the Korean Physical Society, 2012, 61, 1545-1549.	0.7	6
65	Magnetic Sensor-Based Detection of Picoliter Volumes of Magnetic Nanoparticle Droplets in a Microfluidic Chip. Journal of Magnetics, 2012, 17, 302-307.	0.4	12
66	Hybrid AMR/PHR ring sensor. Solid State Communications, 2011, 151, 1248-1251.	1.9	26
67	A facile route to sonochemical synthesis of magnetic iron oxide (Fe3O4) nanoparticles. Thin Solid Films, 2011, 519, 8277-8279.	1.8	60
68	Analytes kinetics in lateral flow membrane analyzed by cTnI monitoring using magnetic method. Sensors and Actuators B: Chemical, 2011, 160, 747-752.	7.8	17
69	Magnetic and electrical properties of bulk BaTiO3+MgFe2O4 composite. Journal of Magnetism and Magnetic Materials, 2011, 323, 564-568.	2.3	27
70	Selective Binding and Detection of Magnetic Labels Using PHR Sensor via Photoresist Micro-Wells. Journal of Nanoscience and Nanotechnology, 2011, 11, 4452-4456.	0.9	8
71	Spin-valve planar Hall sensor for single bead detection. Sensors and Actuators A: Physical, 2010, 157, 42-46.	4.1	43
72	Translocation of bio-functionalized magnetic beads using smart magnetophoresis. Biosensors and Bioelectronics, 2010, 26, 1755-1758.	10.1	32

#	Article	IF	CITATIONS
73	High field-sensitivity planar Hall sensor based on NiFe/Cu/IrMn trilayer structure. Journal of Applied Physics, 2010, 107, .	2.5	43
74	Translocation of magnetic beads using patterned magnetic pathways for biosensing applications. Journal of Applied Physics, 2009, 105, 07B312.	2.5	12
75	Hybrid planar Hall-magnetoresistance sensor based on tilted cross-junction. Journal Physics D: Applied Physics, 2009, 42, 055007.	2.8	17
76	Optimization of Spin-Valve Structure NiFe/Cu/NiFe/IrMn for Planar Hall Effect Based Biochips. IEEE Transactions on Magnetics, 2009, 45, 2378-2382.	2.1	19
77	Magnetic Sensor System Using Asymmetric Giant Magnetoimpedance Head. IEEE Transactions on Magnetics, 2009, 45, 2727-2729.	2.1	36
78	Planar Hall bead array counter microchip with NiFe/IrMn bilayers. Journal of Applied Physics, 2008, 104, .	2.5	19
79	Soft chemical synthesis and characterization of Ni0.65Zn0.35Fe2O4 nanoparticles. Journal of Applied Physics, 2007, 101, 123902.	2.5	32
80	Planar Hall resistance sensor for biochip application. Physica Status Solidi (A) Applications and Materials Science, 2007, 204, 4053-4057.	1.8	16
81	The effect of surface crystalline layers on asymmetric off-diagonal magnetoimpedance in field-annealed CoFeSiB amorphous ribbons. Journal of Magnetism and Magnetic Materials, 2006, 304, e186-e188.	2.3	3
82	Modeling of asymmetric giant magnetoimpedance in amorphous ribbons with a surface crystalline layer. Journal of Magnetism and Magnetic Materials, 2005, 288, 130-136.	2.3	13
83	Influence of current amplitude on asymmetric off-diagonal magnetoimpedance in field-annealed amorphous ribbons. IEEE Transactions on Magnetics, 2005, 41, 3646-3648.	2.1	5
84	Off-diagonal magnetoimpedance in field-annealed Co-based amorphous ribbons. Journal of Applied Physics, 2005, 98, 113908.	2.5	10
85	A model for asymmetric giant magnetoimpedance in field-annealed amorphous ribbons. Applied Physics Letters, 2004, 85, 3507-3509.	3.3	29
86	The role of exchange coupling on the giant magnetoimpedance of annealed amorphous materials. Journal of Magnetism and Magnetic Materials, 2002, 249, 293-299.	2.3	20
87	Novel Planar Hall Sensor for Biomedical Diagnosing Lab-on-a-Chip. , 0, , .		0